

# Certifiable Reachability Learning Using a New Lipschitz Continuous Value Function

Jingqi Li<sup>1</sup>, Donggun Lee<sup>2</sup>, Jaewon Lee<sup>3</sup>, Kris Shengjun Dong<sup>1</sup>, Somayeh Sojoudi<sup>1</sup>, Claire Tomlin<sup>1</sup>

**Abstract**—We propose a new reachability learning framework for high-dimensional nonlinear systems, focusing on *reach-avoid problems*. These problems require computing the *reach-avoid set*, which ensures that all its elements can safely reach a target set despite disturbances within pre-specified bounds. Our framework has two main parts: offline learning of a newly designed reach-avoid value function, and post-learning certification. Compared to prior work, our new value function is Lipschitz continuous and its associated Bellman operator is a contraction mapping, both of which improve the learning performance. To ensure deterministic guarantees of our learned reach-avoid set, we introduce two efficient post-learning certification methods. Both methods can be used online for real-time local certification or offline for comprehensive certification. We validate our framework in a 12-dimensional crazyflie drone racing hardware experiment and a simulated 10-dimensional highway take-over example.

**Index Terms**—Reachability, Machine Learning for Robot Control, Reinforcement Learning

## I. INTRODUCTION

**E**NSURING the safe and reliable operation of robotic systems in uncertain environments is a critical challenge as autonomy is introduced into everyday systems. For instance, we would like humanoid robots to safely work close to humans. As a second example, new concepts for air taxis will need real-time synthesis of safe trajectories in crowded airspace. These safety-critical applications are typically characterized by sequences of tasks, and knowing the set of states from which the task can be safely completed despite unpredictable disturbances is important. Reachability analysis addresses this challenge by determining the *reach-avoid set*—a set of states that can safely reach a target set under all possible disturbances within a specified bound, as well as the corresponding control.

Traditional Hamilton-Jacobi reachability analysis methods [1]–[3] leverage dynamic programming to synthesize the optimal control and a reachability value function, whose sign indicates whether or not a state can safely reach the target set. Though theoretically sound, they suffer from the *curse of dimensionality* [4]: as the system’s dimension increases,

This work was supported by DARPA under the Assured Autonomy (grant FA8750-18-C-0101) and ANSR programs (grant FA8750-23-C-0080), the NASA ULI program in Safe Aviation Autonomy (grant 62508787-176172), and the ONR Basic Research Challenge in Multibody Control Systems (grant N00014-18-1-2214). This work was also supported by U.S. Army Research Laboratory and Research Office (grant W911NF2010219).

<sup>1</sup>J. Li, K. Dong, S. Sojoudi and C. Tomlin are with University of California, Berkeley, CA 94704, USA. jingqili@berkeley.edu, krisdong@berkeley.edu, sojoudi@berkeley.edu, tomlin@berkeley.edu.

<sup>2</sup>D. Lee is with the North Carolina State University, NC 27606, USA. dlee48@ncsu.edu.

<sup>3</sup>J. Lee is with Boson AI, CA 95054, USA. lonj7798@gmail.com.

Digital Object Identifier (DOI): see top of this page.

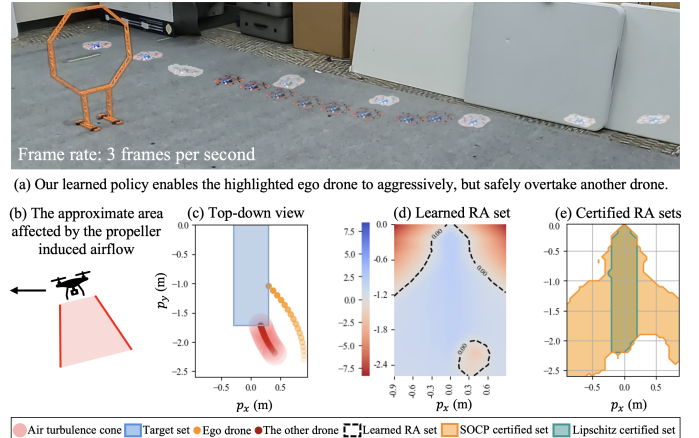


Figure 1: Applying our reachability analysis framework to drone racing. In (a), hardware experiments demonstrate that our learned control policy enables an ego drone to safely overtake another drone, despite unpredictable disturbances in the other drone’s acceleration. In (b), we illustrate the concept of the propeller induced airflow [15], which can affect other drones’ flight. In (c), we apply our learned control policy in a simulation with randomly sampled disturbances. In (d), we project the learned reach-avoid value function onto the  $(x, y)$  position of the ego drone. The super-zero level set, outlined by dashed curves, indicates our learned reach-avoid (RA) set. In (e), we plot the certified RA sets using Lipschitz and second-order cone programming certification.

the computational complexity grows exponentially, making these methods impractical for real-world applications without approximation or further logic to manage the problem size.

There has been interest in using machine learning techniques to estimate reachability value functions for high-dimensional systems [5]–[11]. However, a major drawback of existing reachability learning methods is the lack of deterministic safety guarantees. Recent work [12], [13] provides probabilistic safety guarantees for the learned reach-avoid sets. Additionally, safety filter approaches [10], [11], [14] have been proposed, which offer point-wise guarantees by ensuring safety for individual states.

In this work, we propose the first method for learning reach-avoid sets for high-dimensional nonlinear systems with deterministic assurances. Our method involves learning a new reach-avoid value function (Sections IV and V), and then conducting set-based certification to ensure that all states in the certified set safely reach the target set despite disturbances (Section VI). Specifically:

1) We propose a new reach-avoid value function that is provably Lipschitz continuous. Though it is not based on a Lagrange-type objective function (cumulative rewards over time) as in classical reinforcement learning (RL) [16], we prove its Bellman equation is still a contraction mapping, removing the need for contractive Bellman equation approximation commonly used in prior reachability works [10], [11]. Moreover,

the control policy derived from our value function tends to reach the target set rapidly. We apply deep RL to learn this new value function.

2) We develop two reach-avoid set certification methods. The first uses the Lipschitz constant of the dynamics to certify the safety of a subset of the learned reach-avoid set, ensuring all its elements can safely reach the target set under disturbances. The second employs second-order cone programming to do the same. Both methods offer deterministic assurances. They can be applied online to verify if a neighboring set around the current state can safely reach the target set, or offline for verifying the same for a larger user-defined set.

3) We show the computational benefits of our new value function and the assurance of our (real-time) certification methods through simulations and hardware experiments. We empirically justify that the Lipschitz continuity of our new value function can accelerate value function learning.

## II. RELATED WORKS

**Hamilton-Jacobi reachability learning.** DeepReach [5] is a pioneering work on learning finite-horizon reachability value functions. In other studies, such as [6]–[11], [14], the assumption of a known horizon is relaxed and infinite horizon reachability learning problems are considered. In this work, we also consider the infinite horizon case. We introduce a new value function which is provably Lipschitz continuous and whose Bellman operator is a contraction mapping, offering computational efficiency when compared with prior work.

**Verification of learning-based control.** Recent work [12], [13], [17] has provided probabilistic safety guarantees for DeepReach. In this paper, we introduce methods that provide deterministic reach-avoid guarantees and we show how they could be used locally in real time. Other studies [10], [11], [14] provide point-wise safety filters. However, we propose set-based reach-avoid certification methods to verify if all states in a set can safely reach the target set under potential disturbances. Our certification methods also differ from existing set-based approaches for verifying neural network-controlled systems, including those that verify regions of attraction [18]–[20], forward reachability sets [21]–[25], and safe sets using barrier certificates [26]–[28]. To the best of the authors’ knowledge, our work is the first to certify if a set of initial states is within the ground truth reach-avoid set.

**Constrained optimal control.** Control barrier functions (CBFs) offer safety guarantees [29]–[31], but they tend to be more conservative than model predictive control (MPC) [32], [33], which optimally balances task performance and safety. However, constructing or learning CBFs and solving MPC can be difficult for nonlinear systems with complex constraints. By leveraging deep neural networks, constrained reinforcement learning (CRL) [34]–[36] learns control policies that maximize task rewards while adhering to complex constraints. CBFs, along with the typical value functions defined in MPC and CRL, do not provide the information about whether a state can safely reach the target set. In contrast, our new value function not only provides the optimal control for the worst-case disturbance, but also indicates, based on its sign, whether or not a state can safely reach the target set.

## III. PROBLEM FORMULATION

We consider uncertain nonlinear dynamics described by

$$x_{t+1} = f(x_t, u_t, d_t), \quad (1)$$

where  $x_t \in \mathbb{R}^n$  is the state,  $u_t \in \mathcal{U} \subseteq \mathbb{R}^{m_u}$  is the control, and  $d_t \in \mathcal{D} \subseteq \mathbb{R}^{m_d}$  represents the disturbance, such as model mismatch or uncertain actions of other agents. We assume that both  $\mathcal{U}$  and  $\mathcal{D}$  are compact and connected sets. The disturbance bound could be estimated from prior data or a physical model. We define a state trajectory originating from an initial condition  $x_0$  under a control policy  $\pi : \mathbb{R}^n \rightarrow \mathcal{U}$  and a disturbance policy  $\phi : \mathbb{R}^n \times \mathcal{U} \rightarrow \mathcal{D}$  as  $\xi_{x_0}^{\pi, \phi} := \{x_t\}_{t=0}^{\infty}$ , where  $x_{t+1} = f(x_t, \pi(x_t), \phi(x_t, \pi(x_t)))$ ,  $\forall t \in \{0, 1, 2, \dots\}$ .

Let  $\mathcal{T} \subseteq \mathbb{R}^n$  be an open set, representing a *target set*. We assume that there exists a Lipschitz continuous, bounded reward function  $r : \mathbb{R}^n \rightarrow \mathbb{R}$  indicating if a state  $x$  is in the target set,

$$r(x) > 0 \iff x \in \mathcal{T}. \quad (2)$$

We consider a finite number of Lipschitz continuous, bounded constraint functions  $c_i(x) > 0, \forall i \in \mathcal{I}$ , where  $\mathcal{I}$  is the set of indexes of constraints. Throughout this paper, we define Lipschitz continuity with respect to the  $\ell_2$  norm. We can simplify the representation of constraints by considering their pointwise minimum  $c(x) := \min_{i \in \mathcal{I}} c_i(x)$ . We define the constraint set as  $\mathcal{C} := \{x \in \mathbb{R}^n : c(x) > 0\}$ , and we have

$$c(x) > 0 \iff x \in \mathcal{C}. \quad (3)$$

We look for states that can be controlled to the target set safely under *the worst-case disturbance*, with dynamics given by (1). We refer to this set as the *reach-avoid (RA) set* [2], [37]:

$$\mathcal{R} := \left\{ x_0 : \exists \pi \text{ such that } \forall \phi, \exists T < \infty, \right. \\ \left. (r(x_T) > 0 \wedge \forall t \in [0, T], c(x_t) > 0) \right\}, \quad (4)$$

which includes all the states that can reach the target set safely in finite time despite disturbances within the set  $\mathcal{D}$ .

**Running example, safe take-over in drone racing:** We model the drone take-over example in Figure 1 as an RA problem, where two crazyflie drones [38] compete to fly through an orange gate. The first drone (ego agent) starts behind and aims to overtake the other drone. The second drone flies directly to the gate using an LQR controller, but its acceleration is uncertain to the first drone. We model the uncertain part of the other drone’s acceleration by a disturbance  $\|d_t\|_2 \leq \varepsilon_d := 0.1 \text{ m/s}^2$ . We compute the RA set to ensure the ego drone can safely overtake the other despite this disturbance.

We consider a 12-dimensional dynamics [39], where the  $i$ -th drone’s state is  $x_t^i = [p_{x,t}^i, v_{x,t}^i, p_{y,t}^i, v_{y,t}^i, p_{z,t}^i, v_{z,t}^i]$ . In each of the  $(x, y, z)$  axes, the  $i$ -th drone is modeled by double integrator dynamics, and the control is its acceleration  $u_t^i = [a_{x,t}^i, a_{y,t}^i, a_{z,t}^i]$ , with  $\|u_t^i\|_{\infty} \leq \varepsilon_u := 1 \text{ m/s}^2$ . We model the center of the gate as the origin. The radius of the orange gate is 0.3 meters, and the radius of the crazyflie drone is 0.05 meters. We consider a target set for the ego drone:

$$\mathcal{T} = \left\{ x : \begin{array}{ll} p_y^1 - p_y^2 > 0, & v_y^1 - v_y^2 > 0, \\ |p_x^1| < 0.3, & |p_z^1| < 0.3 \end{array} \right\}. \quad (5)$$

To ensure the ego drone flies through the gate, we constrain:

$$\pm p_{x,t}^1 - p_{y,t}^1 > -0.05, \quad \pm p_{z,t}^1 - p_{y,t}^1 > -0.05. \quad (6)$$

To ensure safe flight, the ego drone should avoid the area affected by the airflow from the other drone, as depicted in Figure 1, using the constraint:

$$\left\| \begin{bmatrix} p_{x,t}^1 - p_{x,t}^2 \\ p_{y,t}^1 - p_{y,t}^2 \end{bmatrix} \right\|_2^2 > \left( 1 + \max(p_{z,t}^2 - p_{z,t}^1, 0) \right) \times 0.2, \quad (7)$$

where the required separation distance between the ego drone and the other drone increases as their height difference grows.

Numerically computing the RA set directly for this problem is computationally infeasible [40]. We introduce our new reachability learning method in the following sections.

#### IV. A NEW REACH-AVOID VALUE FUNCTION

In this section, we propose a new RA value function for evaluating if a state belongs to the RA set. Unlike prior works [6]–[11], [14], our value function incorporates a time-discount factor. This results in a Lipschitz-continuous value function, which appears to accelerate the learning process, and establishes a contractive Bellman equation, eliminating the need for the contractive Bellman equation approximation commonly used in prior works [6]–[11], [14]. Furthermore, we show that the control policy derived from this new value function tends to reach the target set rapidly.

We begin the construction of our new value function by first introducing the concept of *RA measure*, which assesses whether a trajectory can reach the target set safely. Let  $\xi_{x_0}^{\pi, \phi}$  be a trajectory that enters the target set safely at a stage  $t$ . We have  $r(x_t) > 0$  and  $c(x_\tau) > 0$  for all  $\tau \in \{0, 1, \dots, t\}$ . In other words, the *RA measure*  $g(\xi_{x_0}^{\pi, \phi}, t)$ , defined as

$$g(\xi_{x_0}^{\pi, \phi}, t) := \min \left\{ r(x_t), \min_{\tau=0, \dots, t} c(x_\tau) \right\}, \quad (8)$$

is positive,  $g(\xi_{x_0}^{\pi, \phi}, t) > 0$ , if and only if there exists a trajectory from  $x_0$  reaching the target set safely.

An *RA value function*  $\bar{V}(x)$  has been proposed in prior works [6]–[11], [14], and it evaluates the maximum RA measure under the worst-case disturbance:

$$\bar{V}(x) := \max_{\pi} \min_{\phi} \sup_{t=0, \dots} g(\xi_{x_0}^{\pi, \phi}, t), \quad (9)$$

where  $\bar{V}(x) > 0$  if and only if  $x \in \mathcal{R}$ . We compute  $\bar{V}(x)$  by solving its Bellman equation. However,  $\bar{V}(x)$  has a non-contractive Bellman equation, whose solution may not recover  $\mathcal{R}$ , as shown in Figure 2. To address this, prior works [6]–[11], [14] include a time-discount factor  $\gamma$  to create a contractive Bellman equation approximation. For each  $\gamma \in (0, 1)$ , there is a unique solution to the approximated Bellman equation, which converges to  $\bar{V}(x)$  as  $\gamma$  is gradually annealed to 1.

Inspired by previous studies, we enhance computational efficiency by designing a new *time-discounted* RA value function. Ours incorporates a time-discount factor into the value function formulation, resulting in a contractive Bellman equation without the need for any approximation. This improvement eliminates the requirement of the  $\gamma$ -annealing process commonly used in prior works [6]–[11], [14], where  $N$  approximated Bellman equations are solved sequentially with  $\gamma$  values converging to 1. Theoretically, computing our new value function requires only  $\frac{1}{N}$  of the time needed in prior works.

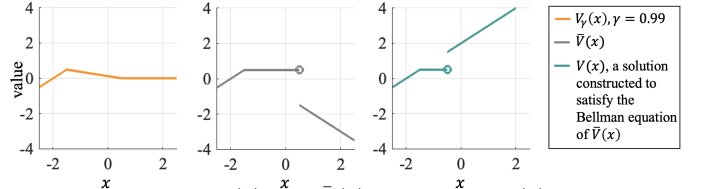


Figure 2: Comparing  $V_\gamma(x)$  with  $\bar{V}(x)$  from (9) and  $V(x)$ , a constructed solution to the Bellman equation of  $\bar{V}(x)$  in prior works [6]–[11], [14]. Consider a 1-dimensional dynamics:  $x_{t+1} = 1.01x_t + 0.01(u_t + d_t)$ , with  $|u_t| \leq 1$  and  $|d_t| \leq 0.5$ . We associate  $\mathcal{T} = \{x : x < -1\}$  and  $\mathcal{C} = \{x : x > -2\}$  with bounded, Lipschitz continuous functions  $r(x) = \max(\min(-x+1), 10), -10$  and  $c(x) = \max(\min(x+2, 10), -10)$ , respectively. For all  $\gamma \in (0, 1)$ , our super-zero level set  $\{x : V_\gamma(x) > 0\}$  equals the RA set  $\mathcal{R} = \{x : -2 < x < 0.5\}$ . By Theorem 2,  $V_\gamma(x)$  is Lipschitz continuous if  $\gamma \in (0, 0.99009)$ . The super-zero level set of  $\bar{V}(x)$  also recovers  $\mathcal{R}$ , but  $\bar{V}(x)$  is discontinuous at  $x = 0.5$  because the control fails to drive the state to  $\mathcal{T}$  under the worst-case disturbance when  $x_t \geq 0.5$ . Finally, in the third subfigure, we show that the Bellman equation in prior works [6]–[11], [14] has non-unique solutions, whose super-zero level set may not equal  $\mathcal{R}$ .

The central part of our new value function is the *time-discounted RA measure*  $g_\gamma(\xi_{x_0}^{\pi, \phi}, t)$ , for a  $\gamma \in (0, 1)$ ,

$$g_\gamma(\xi_{x_0}^{\pi, \phi}, t) := \min \left\{ \gamma^t r(x_t), \min_{\tau=0, \dots, t} \gamma^\tau c(x_\tau) \right\}. \quad (10)$$

This yields a new time-discounted RA value function

$$V_\gamma(x) := \max_{\pi} \min_{\phi} \sup_{t=0, \dots} g_\gamma(\xi_{x_0}^{\pi, \phi}, t). \quad (11)$$

For all  $\gamma \in (0, 1)$  and any finite stage  $t$ , we have

$$g_\gamma(\xi_{x_0}^{\pi, \phi}, t) > 0 \iff g(\xi_{x_0}^{\pi, \phi}, t) > 0. \quad (12)$$

Therefore, for all  $\gamma \in (0, 1)$ , the super-zero level set of  $V_\gamma(x)$ , defined as  $\mathcal{V}_\gamma := \{x : V_\gamma(x) > 0\}$ , is equal to the RA set  $\mathcal{R}$  in (4), and it includes all possible states that can reach the target set safely in finite time under the worst-case disturbance.

In what follows, we present the advantages of our new value function. First, we show that the Bellman equation for  $V_\gamma(x)$  is a contraction mapping, with  $V_\gamma(x)$  as its unique solution.

**Theorem 1** (Contraction mapping). *Let  $\gamma \in (0, 1)$  and  $V : \mathbb{R}^n \rightarrow \mathbb{R}$  be an arbitrary bounded function. Consider the Bellman operator  $B_\gamma[V]$  defined as,*

$$B_\gamma[V](x) := \max_u \min_d \min \{ c(x), \max \{ r(x), \gamma V(f(x, u, d)) \} \}.$$

*Then, we have  $\|B_\gamma[V_\gamma^1] - B_\gamma[V_\gamma^2]\|_\infty \leq \gamma \|V_\gamma^1 - V_\gamma^2\|_\infty$ , for all bounded functions  $V_\gamma^1$  and  $V_\gamma^2$ , and  $V_\gamma(x)$  in (11) is the unique solution to the Bellman equation  $V(x) = B_\gamma[V](x)$ .*

*Proof.* Let  $\pi^*$  and  $\phi^*$  be the optimal control and the worst-case disturbance policies. Observe  $V_\gamma(x_0) = \max_{\pi} \min_{\phi} \min \{ c(x_0), \max \{ r(x_0), \gamma \sup_{\tau=0, \dots} g(\xi_{x_1}^{\pi^*, \phi^*}, \tau) \} \} = \max_{\pi} \min_{\phi} \min \{ c(x_0), \max \{ r(x_0), \gamma V_\gamma(x_1) \} \}$ , where  $x_1 = f(x_0, \pi(x_0), \phi(x_0, \pi(x_0)))$  is the only variable affected by  $\pi$  and  $\phi$ . Following [16, p.234], it can be rewritten as  $V_\gamma(x_0) = \max_{u_0} \min_{d_0} \min \{ c(x_0), \max \{ r(x_0), \gamma V_\gamma(x_1) \} \}$ .

Thus,  $V_\gamma(x)$  is a valid solution to the Bellman equation  $V = B_\gamma[V]$ . We show it is a unique solution by proving that  $B_\gamma[V]$  is a contraction mapping when  $\gamma \in (0, 1)$ , i.e.,  $\|B_\gamma[V_1] - B_\gamma[V_2]\|_\infty \leq \gamma \|V_1 - V_2\|_\infty$ , where  $V_1$  and  $V_2$  are two arbitrary bounded functions. Let  $x$  be an arbitrary state. We have  $\|B_\gamma[V_1](x) - B_\gamma[V_2](x)\|_\infty \leq \|\gamma \max_u \min_d V_1(f(x, u, d)) - \gamma \max_u \min_d V_2(f(x, u, d))\|_\infty$ . Since the max-min operator is non-expansive, we have, for all  $x$ ,  $\|B_\gamma[V_1](x) - B_\gamma[V_2](x)\|_\infty \leq \gamma \|V_1(x) - V_2(x)\|_\infty$ .  $\square$

Theorem 1 suggests that annealing  $\gamma$  to 1 is unnecessary in our method because, for all  $\gamma \in (0, 1)$ , our Bellman equation admits  $V_\gamma(x)$  as the unique solution, and the super-zero level set of  $V_\gamma(x)$  equals the ground truth RA set.

Furthermore, we show in the following result that our new value function can be constructed to be Lipschitz continuous, which facilitates efficient learning when approximating high-dimensional value functions using neural networks [41], [42].

**Theorem 2** (Lipschitz continuity). *Suppose that  $r(\cdot)$  and  $c(\cdot)$  are  $L_r$ - and  $L_c$ -Lipschitz continuous functions, respectively. Assume also that the dynamics  $f(x, u, d)$  is  $L_f$ -Lipschitz continuous in  $x$ , for all  $u \in \mathcal{U}$  and  $d \in \mathcal{D}$ . Let  $L := \max(L_r, L_c)$ . Then,  $V_\gamma(x)$  is  $L$ -Lipschitz continuous if  $\gamma L_f < 1$ .*

*Proof.* Consider two arbitrary initial states  $x_0, x'_0 \in \mathbb{R}^n$ . Let  $\pi^*$  and  $\phi^*$  be the optimal control and the worst-case disturbance policies. For each  $t \in \{0, 1, 2, \dots\}$ , define  $x_{t+1} := f(x_t, u_t, d'_t)$ ,  $u_t := \pi^*(x_t)$ ,  $x'_{t+1} := f(x'_t, u_t, d'_t)$ , and  $d'_t := \phi^*(x'_t, u_t)$ . Let  $\mathbf{u} := \{u_t\}_{t=0}^\infty$ ,  $\mathbf{d}' := \{d'_t\}_{t=0}^\infty$ ,  $\mathbf{x} := \{x_t\}_{t=0}^\infty$ , and  $\mathbf{x}' := \{x'_t\}_{t=0}^\infty$ . Given an arbitrarily small  $\varepsilon > 0$ , there exists a  $\bar{t} < \infty$  such that  $V_\gamma(x_0) \leq g_\gamma(\mathbf{x}, \bar{t}) + \varepsilon$ . By definition, we have  $V_\gamma(x'_0) \geq g_\gamma(\mathbf{x}', \bar{t})$ . Combining two inequalities, we have  $V_\gamma(x'_0) - V_\gamma(x_0) + \varepsilon \geq \min\{\gamma^{\bar{t}}(r(x'_\bar{t}) - r(x_\bar{t})), \min_{\tau=0, \dots, \bar{t}} \gamma^\tau (c(x'_\tau) - c(x_\tau))\} \geq -\max\{L_r \gamma^{\bar{t}} L_f^{\bar{t}}, \max_{\tau=0, \dots, \bar{t}} L_c \gamma^\tau L_f^\tau\} \|x_0 - x'_0\|_2$ . The condition  $\gamma L_f < 1$  implies  $(\gamma L_f)^{\bar{t}} < 1$ ,  $\forall \bar{t}$ . As a result,  $V_\gamma(x'_0) - V_\gamma(x_0) + \varepsilon \geq -L \|x_0 - x'_0\|_2$ . Similarly, we can show that  $V_\gamma(x_0) - V_\gamma(x'_0) + \varepsilon \geq -L \|x_0 - x'_0\|_2$ . Combining these two inequalities, we prove Theorem 2.  $\square$

The main idea of the proof is that a small perturbation in the state  $x$  leads to a bounded change of the time-discounted RA measure value. Theorem 2 suggests that we can ensure the Lipschitz continuity of  $V_\gamma(x)$  by selecting  $\gamma < \frac{1}{L_f}$ . In contrast, the classical RA value function  $\bar{V}(x)$  can be discontinuous, as shown in Figure 2.

Moreover, the control policy derived from  $V_\gamma(x)$  reaches the target set quickly, as a trajectory that reaches the target set rapidly incurs a high time-discounted RA measure value.

**Theorem 3** (Fast reaching). *Let  $x$  be in the RA set and  $\phi$  be an arbitrary disturbance policy. Let  $\gamma \in (0, 1)$ . Suppose  $(\pi_1, t_1)$  and  $(\pi_2, t_2)$  are two control policies and corresponding times to maximize the discounted RA measure  $g_\gamma$ ,  $(\pi_1, t_1), (\pi_2, t_2) \in \arg \max_{\pi, t} g_\gamma(\xi_x^{\pi, \phi}, t)$ . Moreover, suppose  $t_1 < t_2$ , then for all  $\tilde{\gamma} \in (0, \min\{\gamma, \frac{V_\gamma(x)}{\max_x r(x)}\})$ , we have  $g_{\tilde{\gamma}}(\xi_x^{\pi_2, \phi}, t_2) < g_{\tilde{\gamma}}(\xi_x^{\pi_1, \phi}, t_1)$ .*

*Proof.* From the definitions of  $\tilde{\gamma}$ ,  $g_\gamma$ , and  $V_\gamma(x)$ , and the boundedness of  $r(x)$ , we have  $\tilde{\gamma} < 1$ , and  $g_{\tilde{\gamma}}(\xi_x^{\pi_2, \phi}, t_2) \leq \tilde{\gamma}^{t_1} \tilde{\gamma} \max_x r(x) \leq \tilde{\gamma}^{t_1} V_\gamma(x) < (\frac{\tilde{\gamma}}{\gamma})^{t_1} V_\gamma(x) \leq (\frac{\tilde{\gamma}}{\gamma})^{t_1} g_\gamma(\xi_x^{\pi_1, \phi}, t_1) \leq g_{\tilde{\gamma}}(\xi_x^{\pi_1, \phi}, t_1)$ .  $\square$

Theorem 3 also suggests that a control policy reaching the target set slowly may become suboptimal when  $\gamma$  is decreased.

While a small time-discount factor in  $V_\gamma(x)$  offers numerous benefits, it is not conclusive that  $\gamma$  should always be near zero. In theory, for all  $\gamma \in (0, 1)$ , the super-zero level set of  $V_\gamma(x)$  recovers the exact RA set. However, in practice, a near-zero

$\gamma$  can lead to a conservatively estimated RA set, where a trajectory reaching the target set at a late stage may have a near-zero or even negative time-discounted RA measure due to numerical errors. We will explore the trade-offs of selecting various  $\gamma$  values in Section VIII-D.

## V. LEARNING THE NEW RA VALUE FUNCTION

Since the optimal RA control policy is deterministic [37], we adapt max-min Deep Deterministic Policy Gradient (DDPG) [43], a deep RL method for learning deterministic policies and their value functions, to learn  $\pi$ ,  $\phi$  and  $V_\gamma$ .

Let  $\gamma$  be an arbitrary time discount factor in  $(0, 1)$ . Similar to prior works [10], [11], [14], we approximate the optimal control policy  $\pi^*(x)$  and the worst-case disturbance policy  $\phi^*(x, \pi^*(x))$  by neural network (NN) policies  $\pi_{\theta_u}(x)$  and  $\phi_{\theta_d}(x)$ , respectively, with  $\theta_u$  and  $\theta_d$  being their parameters. We define an NN Q function as  $Q_{\theta_q} : \mathbb{R}^n \times \mathcal{U} \times \mathcal{D} \rightarrow \mathbb{R}$ , where  $\theta_q$  represents the NN's parameter vector. Substituting  $\pi_{\theta_u}$  and  $\phi_{\theta_d}$  into  $Q_{\theta_q}$ , we can derive an NN value function  $V_\theta(x) := Q_{\theta_q}(x, \pi_{\theta_u}(x), \phi_{\theta_d}(x))$ , where  $\theta$  is the concatenation of parameters  $\theta_q$ ,  $\theta_u$  and  $\theta_d$ . Let  $\mathbb{P}$  be a sampling distribution with a sufficiently large support in  $\mathbb{R}^n$  that covers at least a part of the target set. In max-min DDPG, we learn  $\pi_{\theta_u}$ ,  $\phi_{\theta_d}$  and  $Q_{\theta_q}$  by alternatively optimizing the following problems:

We learn  $\pi_{\theta_u}$  by maximizing the Q value over  $\theta_u$ :

$$\max_{\theta_u} \mathbb{E}_{x \sim \mathbb{P}} Q_{\theta_q}(x, \pi_{\theta_u}(x), \phi_{\theta_d}(x)). \quad (13)$$

We learn  $\phi_{\theta_d}$  by minimizing the Q value over  $\theta_d$ :

$$\min_{\theta_d} \mathbb{E}_{x \sim \mathbb{P}} Q_{\theta_q}(x, \pi_{\theta_u}(x), \phi_{\theta_d}(x)). \quad (14)$$

We learn  $Q_{\theta_q}$  by minimizing the *critic loss*, also known as the Bellman equation error, over  $\theta_q$ :

$$\min_{\theta_q} \mathbb{E}_{x \sim \mathbb{P}} \|V_\theta(x) - B_\gamma[V_\theta(x)]\|_2^2. \quad (15)$$

We define the *learned RA set*  $\hat{\mathcal{R}}$  as the super zero-level set of  $V_\theta(x)$ . When DDPG converges to an optimal solution,  $V_\theta(x)$  converges to  $V_\gamma(x)$  due to Theorem 1. However, in practice, like other deep RL methods, DDPG often converges to a suboptimal solution with a near-zero critic loss. When  $V_\theta(x)$  is a suboptimal solution,  $\hat{\mathcal{R}}$  cannot be reliably considered as the ground truth RA set  $\mathcal{R}$ . This motivates us to use a suboptimal learning result to certify a trustworthy RA set, as detailed in the following section.

## VI. CERTIFYING RA SETS WITH GUARANTEES

In this section, we propose two methods to certify if a set of states belongs to the ground truth RA set. Both methods use a learned control policy, which is not necessarily optimal.

### A. Certification using Lipschitz constants

We leverage a learned control policy  $\pi_{\theta_u}$  and the Lipschitz constants of dynamics, reward and constraint to construct a theoretical lower bound of the ground truth value function  $V_\gamma(x)$ . *If such a lower bound of  $V_\gamma(x)$  is greater than zero for all states in the neighboring set of  $x_0$ ,  $\mathcal{E}_{x_0} := \{x : \|x - x_0\|_2 \leq \varepsilon_x\}$ , then  $V_\gamma(x) > 0$ ,  $\forall x \in \mathcal{E}_{x_0}$ . We claim that the set  $\mathcal{E}_{x_0}$  is within the ground truth RA set  $\mathcal{R}$ .*

We begin constructing a lower bound of  $V_\gamma(x)$  by considering a  $T$ -stage, disturbance-free, nominal trajectory  $\{\bar{x}_t\}_{t=0}^T$ ,

$$\bar{x}_{t+1} = f(\bar{x}_t, \bar{u}_t, 0), \bar{u}_t = \pi_{\theta_u}(\bar{x}_t), \quad \forall t = 0, \dots, T-1 \quad (16)$$

and a disturbed state trajectory  $\{\tilde{x}_t\}_{t=0}^T$  under  $\{\tilde{u}_t\}_{t=0}^{T-1}$  using an arbitrary  $d_t \in \mathcal{D}$ ,  $\forall t = 0, \dots, T-1$ :

$$\tilde{x}_{t+1} = f(\tilde{x}_t, \tilde{u}_t, d_t), \quad \forall t = 0, \dots, T-1. \quad (17)$$

Note that if we can verify that a trajectory starting at state  $x$  reaches the target set safely despite disturbances within  $T$  stages, then it suffices to claim  $x \in \mathcal{R}$ , where the certification horizon  $T$  can be set arbitrarily. Ideally, we would set  $T = \infty$ , but it is impractical to evaluate an infinitely long trajectory. Therefore, during certification, we consider a finite, user-defined  $T$ . This  $T$  should preferably be long enough to allow initial states to reach the target set. A short  $T$  results in a conservative certification since it overlooks the possibility that the trajectory might safely reach the target set at a later time.

We assume that the dynamics  $f$  is Lipschitz continuous and there exists an upper bound on the disturbance in  $\mathcal{D}$  at each stage  $t$ , i.e.,  $\|d_t\|_2 \leq \varepsilon_d$ . Let  $L_{f_x}$  and  $L_{f_d}$  be the Lipschitz constants of the dynamics  $f$  with respect to the state  $x$  and disturbance  $d$ , respectively. At time  $t = 1$ , we observe

$$\begin{aligned} \|\bar{x}_1 - \tilde{x}_1\|_2 &= \|f(\bar{x}_0, \bar{u}_0, 0) - f(\tilde{x}_0, \bar{u}_0, d_0)\|_2 \\ &\leq L_{f_x} \|\bar{x}_0 - \tilde{x}_0\|_2 + L_{f_d} \|0 - d_0\|_2 \leq L_{f_x} \varepsilon_x + L_{f_d} \varepsilon_d. \end{aligned}$$

At time  $t = 2$ ,

$$\begin{aligned} \|\bar{x}_2 - \tilde{x}_2\|_2 &= \|f(\bar{x}_1, \bar{u}_1, 0) - f(\tilde{x}_1, \bar{u}_1, d_1)\|_2 \\ &\leq L_{f_x} \|\bar{x}_1 - \tilde{x}_1\|_2 + L_{f_d} \varepsilon_d. \end{aligned}$$

By induction, we have

$$\|\bar{x}_t - \tilde{x}_t\|_2 \leq L_{f_x}^t \varepsilon_x + \sum_{\tau=0}^{t-1} L_{f_x}^\tau L_{f_d} \varepsilon_d =: \Delta x_t. \quad (18)$$

We define a convex outer approximation of the set of dynamically feasible states as  $\mathcal{X}_{t, \bar{x}_0}^L := \{x_t : \|x_t - \bar{x}_t\|_2 \leq \Delta x_t\}$ , and we check if for all  $x_t \in \mathcal{X}_{t, \bar{x}_0}^L$ ,  $r(x_t) > 0$  and  $c(x_t) > 0$ . By Lipschitz continuity of the reward function, we have,

$$\forall x_t \in \mathcal{X}_{t, \bar{x}_0}^L, \quad \|r(\bar{x}_t) - r(x_t)\|_2 \leq L_r \Delta x_t$$

which yields a lower bound of  $r(x_t)$ , for all  $x_t \in \mathcal{X}_{t, \bar{x}_0}^L$ :

$$\check{r}_t^L := r(\bar{x}_t) - L_r \Delta x_t \leq r(x_t). \quad (19)$$

Similarly, we have a lower bound of  $c(x_t)$ , for all  $x_t \in \mathcal{X}_{t, \bar{x}_0}^L$ :

$$\check{c}_t^L := c(\bar{x}_t) - L_c \Delta x_t \leq c(x_t). \quad (20)$$

Using  $\check{r}_t^L$  and  $\check{c}_t^L$ , we can construct a lower bound  $\check{V}_\gamma^L(\bar{x}_0, T)$  for  $V_\gamma(x_0)$ , for all  $x_0 \in \mathcal{E}_{\bar{x}_0}$ :

$$\check{V}_\gamma^L(\bar{x}_0, T) := \max_{t=0, \dots, T} \min \{ \gamma^t \check{r}_t^L, \min_{\tau=0, \dots, t} \gamma^\tau \check{c}_\tau^L \} \leq V_\gamma(x_0). \quad (21)$$

This implies

$$\check{V}_\gamma^L(\bar{x}_0, T) > 0 \implies V_\gamma(x_0) > 0, \forall x_0 \in \mathcal{E}_{\bar{x}_0}. \quad (22)$$

Thus, when  $\check{V}_\gamma^L(\bar{x}_0, T) > 0$ , the set  $\mathcal{E}_{\bar{x}_0}$  is *certified* to be within the ground truth RA set  $\mathcal{R}$ . Moreover,  $\{\tilde{u}_t\}_{t=0}^{T-1}$  are the *certified control inputs* that can drive all  $x \in \mathcal{E}_{\bar{x}_0}$  to the target set  $\mathcal{T}$  safely despite disturbances in  $\mathcal{D}$ .

## B. Certification using second-order cone programming

Lipschitz certification is fast to compute. However, the lower bound  $\check{V}_\gamma^L$  can be conservative. In this subsection, we propose another certification method using second-order cone programming (SOCP), aiming to provide a less conservative RA certification. Our key idea is to construct SOCPs that search over a tight, convex outer approximation set of the dynamically feasible trajectories and verify whether the state trajectory reaches the target set safely under all disturbances, within a user-defined finite certification horizon  $T$ .

The construction of these SOCPs involves two steps.

First, we formulate a *surrogate RA problem*: A subset of the original target set  $\mathcal{T}$ , represented by the interior of a polytope  $\check{\mathcal{T}} := \{x : P_i x - k_i > 0, i \in \mathcal{I}_{\check{\mathcal{T}}}\}$ , is defined as a *surrogate target set*  $\check{\mathcal{T}}$ , where  $\mathcal{I}_{\check{\mathcal{T}}}$  is a finite index set of the polytope's edges. Additionally, we define a subset of the original constraint set  $\mathcal{C}$ , represented by the intersection of a finite number of positive semidefinite quadratic functions' super-zero level sets  $\check{\mathcal{C}} := \{x : \frac{1}{2} x^\top Q_i x + q_i^\top x + b_i > 0, i \in \mathcal{I}_{\check{\mathcal{C}}}\}$ , as a *surrogate (nonconvex) constraint set*  $\check{\mathcal{C}}$ . The set  $\check{\mathcal{C}}$  could be nonconvex when approximating collision avoidance constraints.

Subsequently, we leverage SOCPs to verify if a state trajectory from  $x_0$  can reach  $\check{\mathcal{T}}$  while staying within  $\check{\mathcal{C}}$  despite disturbances. We achieve this by sequentially minimizing each function defined in  $\check{\mathcal{T}}$  and  $\check{\mathcal{C}}$ , iterating from the stage  $\tau = 0$  to  $\tau = T$ . *If their minimum is positive at a stage  $t$  and there is no intermediate stage  $\tau < t$  such that  $x_\tau$  is outside  $\check{\mathcal{C}}$ , we claim that the initial state  $x_0$  can safely reach the original target set  $\mathcal{T}$ , under all possible disturbances.*

To be more specific, we can check if there exists a stage  $t \in \{0, 1, \dots, T\}$  such that, for all disturbances, all dynamically feasible states  $x_t$ , originating from the initial states set  $\mathcal{E}_{\bar{x}_0} := \{x : \|x - \bar{x}_0\|_2 \leq \varepsilon_x\}$ , are within  $\check{\mathcal{T}}$  and for all stages  $\tau \leq t$ ,  $x_\tau$  are within  $\check{\mathcal{C}}$ . If this condition is met, we claim that  $\mathcal{E}_{\bar{x}_0}$  is within the ground truth RA set  $\mathcal{R}$ , i.e.,  $\mathcal{E}_{\bar{x}_0} \subseteq \mathcal{R}$ . Otherwise, some of its elements could be outside  $\mathcal{R}$ , and therefore we do not claim  $\mathcal{E}_{\bar{x}_0} \subseteq \mathcal{R}$ . To make the analysis tractable, we define the nominal state trajectory  $\{\bar{x}_t\}_{t=0}^T$  and nominal control trajectory  $\{\bar{u}_t\}_{t=0}^{T-1}$  as in (16). The nominal state and control trajectories allow us to formulate a convex set  $\mathcal{X}_{t, \bar{x}_0}^S$  for outer approximating the set of dynamically feasible states:

$$\begin{aligned} \mathcal{X}_{t, \bar{x}_0}^S &:= \{x_t : \exists \{d_\tau\}_{\tau=0}^{t-1} \text{ and } x_0 \text{ such that } \forall \tau \leq t-1, \\ x_{\tau+1} &\leq \hat{A}_\tau x_\tau + \hat{B}_\tau \bar{u}_\tau + \hat{D}_\tau d_\tau + \hat{c}_\tau, \text{ (Upper bound on } f) \\ x_{\tau+1} &\geq \check{A}_\tau x_\tau + \check{B}_\tau \bar{u}_\tau + \check{D}_\tau d_\tau + \check{c}_\tau, \text{ (Lower bound on } f) \\ \|d_\tau\|_2 &\leq \varepsilon_d, \text{ (Disturbance bound)} \\ \|x_0 - \bar{x}_0\|_2 &\leq \varepsilon_x \text{ (Initial state bound)} \end{aligned}$$

where the first two inequalities are element-wise and the bounds on the dynamics  $f$  can be derived using its Lipschitz constant or a Taylor series<sup>1</sup>. At a stage  $t$ , we can verify if  $x_t \in \check{\mathcal{T}}$  by solving a sequence of SOCPs iterating over all  $i \in \mathcal{I}_{\check{\mathcal{T}}}$ , and checking if their minimum is positive:

$$\check{r}_t^S := \min_{i \in \mathcal{I}_{\check{\mathcal{T}}}} \left\{ \min_{x_t \in \mathcal{X}_{t, \bar{x}_0}^S} P_i x_t - k_i \right\}. \quad (23)$$

<sup>1</sup>For simplicity, we can also use  $\mathcal{X}_{t, \bar{x}_0}^L$  to define the convex outer approximation set of the dynamically feasible states in SOCP certifications, i.e.,  $\mathcal{X}_{t, \bar{x}_0}^S := \mathcal{X}_{t, \bar{x}_0}^L$ .

Similarly, for checking whether  $x_t \in \tilde{\mathcal{C}}$ , we can evaluate if the following term is positive:

$$\check{c}_t^S := \min_{i \in \mathcal{I}_{\tilde{\mathcal{C}}}} \left\{ \min_{x_t \in \mathcal{X}_{t,\bar{x}_0}^S} \frac{1}{2} x_t^\top Q_i x_t + q_i^\top x_t + b_i \right\}. \quad (24)$$

Combining the above two terms, we can construct a conservative certificate  $\check{V}_\gamma^S$  for verifying if a state  $\bar{x}_0$  and its neighboring set  $\mathcal{E}_{\bar{x}_0}$  are within the ground truth RA set  $\mathcal{R}$ ,

$$V_\gamma^S(\bar{x}_0, T) := \max_{t=0, \dots, T} \min \{ \gamma^t \check{r}_t^S, \min_{\tau=0, \dots, t} \gamma^\tau \check{c}_\tau^S \}. \quad (25)$$

This suggests

$$\check{V}_\gamma^S(\bar{x}_0, T) > 0 \implies V_\gamma(x_0) > 0, \forall x_0 \in \mathcal{E}_{\bar{x}_0} \quad (26)$$

and  $\{\bar{u}_t\}_{t=0}^{T-1}$  are the *certified control inputs*, capable of driving all  $x \in \mathcal{E}_{\bar{x}_0}$  to the target set  $\mathcal{T}$  safely despite disturbances.

**Running example (continued).** At stage  $t$ , we evaluate  $\check{r}_t^S = \min_i \{\check{r}_{t,i}^S\}_{i=1}^6$  by solving the following SOCPs, where each  $\check{r}_{t,i}^S$  corresponds a function in the definition of  $\mathcal{T}$  in (5):

$$\check{r}_{t,1}^S = \min_{x_t \in \mathcal{X}_{t,\bar{x}_0}^S} p_{y,t}^1 - p_{y,t}^2, \quad \check{r}_{t,2}^S = \min_{x_t \in \mathcal{X}_{t,\bar{x}_0}^S} v_{y,t}^1 - v_{y,t}^2$$

$$\check{r}_{t,3}^S = \min_{x_t \in \mathcal{X}_{t,\bar{x}_0}^S} 0.3 - p_{x,t}^1, \quad \check{r}_{t,4}^S = \min_{x_t \in \mathcal{X}_{t,\bar{x}_0}^S} 0.3 + p_{x,t}^1$$

$$\check{r}_{t,5}^S = \min_{x_t \in \mathcal{X}_{t,\bar{x}_0}^S} 0.3 - p_{z,t}^1, \quad \check{r}_{t,6}^S = \min_{x_t \in \mathcal{X}_{t,\bar{x}_0}^S} 0.3 + p_{z,t}^1$$

Similarly, we can evaluate  $\check{c}_t^S = \min_i \{\check{c}_{t,i}^S\}_{i=1}^5$  by considering the following SOCPs, where each  $\check{c}_{t,i}^S$  corresponds to a constraint function in (6) and (7):

$$\check{c}_{t,i}^S = \min_{x_t \in \mathcal{X}_{t,\bar{x}_0}^S} (-1)^i \times p_{x,t}^1 - p_{y,t}^1 + 0.05, \quad i \in \{1, 2\},$$

$$\check{c}_{t,i}^S = \min_{x_t \in \mathcal{X}_{t,\bar{x}_0}^S} (-1)^i \times p_{z,t}^1 - p_{y,t}^1 + 0.05, \quad i \in \{3, 4\}.$$

We overapproximate the maximum height difference between two drones via  $\Delta_{z,t}^{21} := \max_{x_t \in \mathcal{X}_{t,\bar{x}_0}^S} p_{z,t}^2 - p_{z,t}^1$ , and consider

$$\check{c}_{t,5}^S = \min_{x_t \in \mathcal{X}_{t,\bar{x}_0}^S} \left\| \begin{bmatrix} p_{x,t}^1 - p_{x,t}^2 \\ p_{y,t}^1 - p_{y,t}^2 \end{bmatrix} \right\|_2^2 - (1 + \max(\Delta_{z,t}^{21}, 0)) \times 0.2$$

**Remark 1.** 1) *SOCP certification can be less conservative than Lipschitz certification when  $\tilde{\mathcal{T}}$  and  $\tilde{\mathcal{C}}$  can represent  $\mathcal{T}$  and  $\mathcal{C}$  exactly, and  $\mathcal{X}_{t,\bar{x}_0}^S$  is a subset of the Lipschitz dynamically feasible set  $\mathcal{X}_{t,\bar{x}_0}^L$ , as defined in Section VI-A, for all  $t \leq T$ . This is because Lipschitz certification adds extra conservatism when estimating lower bounds of  $r(x)$  and  $c(x)$  using the Lipschitz constant, as shown in (19) and (20); 2) However, Lipschitz certification is faster to compute than SOCP because calculating  $\check{r}_t^L$  and  $\check{c}_t^L$  is easier than evaluating  $\check{r}_t^S$  and  $\check{c}_t^S$ ; 3) SOCP certification employs convex over-approximations of the dynamically feasible state sets, similar to tube MPC [33]. However, it differs from tube MPC in that we compute the worst-case (nonconvex) constraint violation and target set deviation rather than the control inputs that optimize an objective.*

**Remark 2.** *The computational complexity of evaluating  $\check{V}_\gamma^L(x, T)$  and  $\check{V}_\gamma^S(x, T)$  scales **polynomially** with both the dimension of the dynamical system and the length of  $T$ .*

## VII. COMBINING REACHABILITY LEARNING AND CERTIFICATION

We integrate the reachability learning and certification into a new framework of computing trustworthy RA sets, as described in Algorithm 1. The super zero-level set of  $V_\theta$  provides an

---

### Algorithm 1: Certifiable Reachability Learning:

---

**Require:** an arbitrary  $\gamma \in (0, 1)$ , a finite list of states  $\mathcal{L}$ , and a certification horizon  $T < \infty$ ;  
**Initialization:** certified RA set  $\mathcal{S} \leftarrow \{\}$ ;  
 Learn  $\pi_{\theta_u}$ ,  $\phi_{\theta_d}$  and  $V_\theta$  via max-min DDPG [43];  
 // Certifications:  
**for**  $x_0 \in \mathcal{L}$  **do**  
 | **if**  $\check{V}_\gamma^L(x_0, T) > 0$  or  $\check{V}_\gamma^S(x_0, T) > 0$  **then**  
 | |  $\mathcal{S} \leftarrow \mathcal{S} \cup \{x : \|x_0 - x\|_2 \leq \varepsilon_x\}$   
**return** certified RA set  $\mathcal{S}$

---

estimation of the ground truth RA set. We use  $\pi_{\theta_u}$  to certify a set of states, ensuring deterministic RA guarantees there. In particular, we can apply certification either online or offline:

**Online certification:** Let  $x$  be an arbitrary state. We can use the RA certificates  $\check{V}_\gamma^L(x, T)$  in (21) or  $\check{V}_\gamma^S(x, T)$  in (25) as online RA certification methods, verifying if all elements in  $\mathcal{E}_x = \{x' : \|x' - x\|_2 \leq \varepsilon_x\}$  can reach the target set safely despite disturbances. We can compute  $\check{V}_\gamma^L(x, T)$  and  $\check{V}_\gamma^S(x, T)$  in real-time (10 Hz in our examples), as shown in Figure 5. It can also be integrated into the safety filter proposed in [10], offering more robust RA certification than [10] by verifying that all states in  $\mathcal{E}_x$  can reach the target set safely, thereby enabling RA capability verification without perfect state estimation.

**Offline certification:** We consider a finite set of states  $\mathcal{L} := \{x^{(i)}\}_{i=1}^N$  such that the union of their neighboring sets  $\mathcal{E}_{x^{(i)}} = \{x : \|x - x^{(i)}\|_2 \leq \varepsilon_x\}$  covers the set of states that we aim at certifying. For example, this includes the area near the orange gate in drone racing, as show in Figure 1. We enumerate each element  $x \in \mathcal{L}$  and certify whether  $\mathcal{E}_x \subseteq \mathcal{R}$  by checking if  $\check{V}_\gamma^L$  in (21) or  $\check{V}_\gamma^S$  in (25) is positive. The union  $\mathcal{S}$  of those certified sets constitutes a subset of the ground truth RA set  $\mathcal{R}$ . For all elements in  $\mathcal{S}$ , we guarantee that they can reach the target set safely under potential disturbances.

## VIII. EXPERIMENTS

We test our reachability learning and certification methods<sup>2</sup> in a 12-dimensional drone racing hardware experiment (Figure 3), and a triple-vehicle highway take-over simulation. In the highway simulation, we control one ego vehicle, modeled with nonlinear unicycle dynamics, to safely overtake another vehicle while avoiding a third vehicle driving in the opposite direction, as shown in Figure 4. Figures 1 and 4 demonstrate the high quality of the learned and certified RA sets.

*A. Hypothesis 1: Our learned policy has a higher success rate than state-of-the-art constrained RL methods*

We compare our learned policy  $\pi_{\theta_u}$  with Deep Deterministic Policy Gradient-Lagrangian (DDPG-L) [35], Soft Actor Critic-Lagrangian (SAC-L) [36], and Constrained Policy Optimization (CPO) [34]. We summarize the results in Table I. The success rate is estimated by computing the ratio of sampled initial states that can reach the target set safely under randomly generated

<sup>2</sup>Experiment code and hardware drone racing video are available at [https://github.com/jamesjingqili/Lipschitz\\_Continuous\\_Reachability\\_Learning.git](https://github.com/jamesjingqili/Lipschitz_Continuous_Reachability_Learning.git).

Initial states uniform sampling	Drone racing			Highway			
	DDPG-L	SAC-L	Ours	DDPG-L	SAC-L	CPO	Ours
In a large bounded state set	0.5716	0.7291	<b>0.7655</b>	0.7512	0.6343	0.5552	<b>0.8782</b>
In the learned reach-avoid set	0.6276	0.8006	<b>0.8889</b>	0.9430	0.9149	0.9566	<b>0.9924</b>
In the SOCP certified set	0.9673	0.9948	<b>1.0000</b>	0.9111	0.8850	0.9451	<b>1.0000</b>

Table I: Success rates table. Our method achieves a 1.0 success rate when the initial states are sampled from the SOCP certified set. CPO fails to converge for the drone racing experiment due to the complex and nonconvex constraints.



(a) Ego drone's initial  $(x, y, z)$  position:  $(-0.5, -2.5, 0.0)$  (b) Ego drone's initial  $(x, y, z)$  position:  $(0.9, -2.3, 0.0)$

Figure 3: We sampled 50 initial states from the SOCP certified set shown in Figure 1. A few crashes occurred due to insufficient battery charge or Vicon sensor failures caused by natural light. These instances were excluded as outliers. With a fully charged battery and no Vicon system failures, the ego drone successfully overtook the other drone from each of the 50 initial states, despite the latter's uncertain acceleration. We visualize two hardware experiments in the above subfigures. The remaining 9-dimensional initial state includes  $[v_{x,t}^1, v_{y,t}^1, v_{z,t}^1, p_{x,t}^2, p_{y,t}^2, p_{z,t}^2, v_{x,t}^2, v_{y,t}^2, v_{z,t}^2] = [0, 0.7, 0, 0.4, -2.2, 2, 0, 0.3, 0]$ .

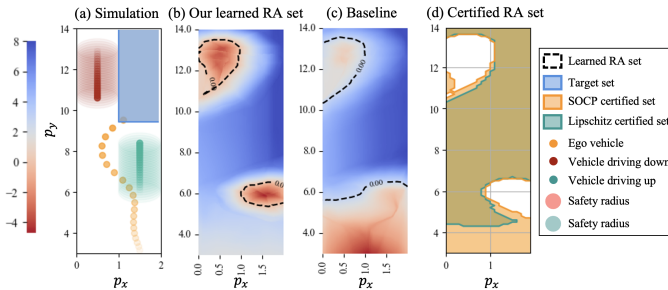


Figure 4: Highway reachability analysis: In (a), we simulate the nonlinear dynamics with the learned policy  $\pi_{\theta_u}$  and randomly sampled disturbances on other vehicles' acceleration. The 10-dimensional state space includes  $[p_{x,t}^1, p_{y,t}^1, v_t^1, \theta_t^1, p_{x,t}^2, p_{y,t}^2, v_{y,t}^2, p_{x,t}^3, p_{y,t}^3, v_{y,t}^3]$ . The  $p_y$ -axis movement of the red and green agents is modeled using double integrator dynamics, while their initial  $p_x$  positions are sampled randomly and remain stationary during simulation. In (b), we project our learned value function, with  $\gamma = 0.95$ , onto the  $(x, y)$  position of the ego vehicle. In (c), we plot the RA set learned using the state-of-the-art method [11], [14] with  $\gamma = 0.95$ . As suggested in [7], annealing  $\gamma \rightarrow 1$  is necessary for prior works; otherwise, the learned RA sets in prior works are conservative. In (d), we plot our certified RA sets.

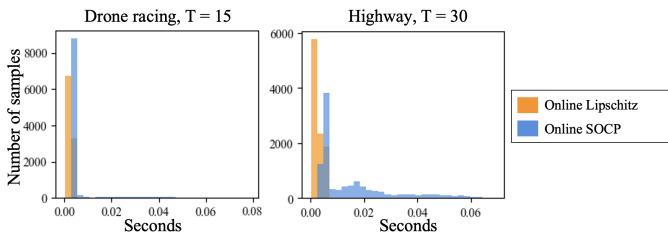


Figure 5: Histogram of the time required for computing  $\check{V}_\gamma^L(x, T)$  and  $\check{V}_\gamma^S(x, T)$  for each of the 10,000 randomly sampled states  $x$ . The certification horizons for drone racing and highway are  $T = 15$  and  $T = 30$ , respectively.

disturbances. Our method achieves a 1.0 success rate when the initial states are sampled from the SOCP certified set, validating the deterministic guarantee that all elements in the certified sets can safely reach the target set despite disturbances.

### B. Hypothesis 2: Our online RA set certification methods can be computed in real-time

Figure 5 shows that  $\check{V}_\gamma^L(x, T)$  and  $\check{V}_\gamma^S(x, T)$  can be computed in real-time to certify if all elements in  $\mathcal{E}_x = \{x' : \|x' -$

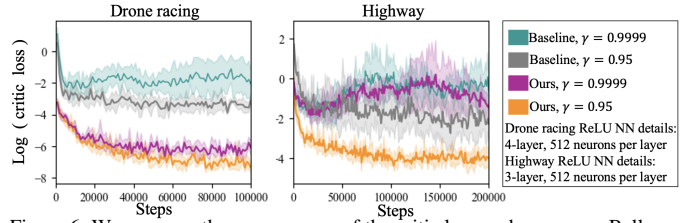


Figure 6: We compare the convergence of the critic loss under our new Bellman equation with the baseline from previous works [11], [14], using different  $\gamma$  values but identical training parameters. Our critic loss with  $\gamma = 0.95$  converges faster than with  $\gamma = 0.9999$ , likely due to the Lipschitz continuity of  $V_\gamma(x)$  at  $\gamma = 0.95$ . The training speed is around 1700 steps per second.

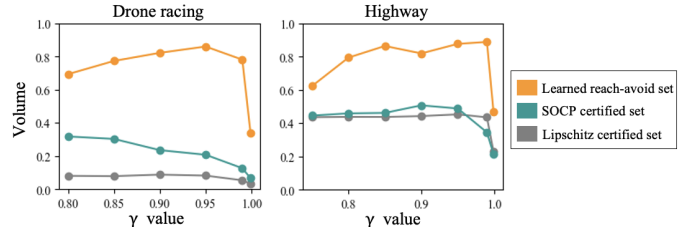


Figure 7: The volumes of the learned RA set, SOCP certified set, and the Lipschitz certified set change as  $\gamma$  varies. We estimate the set volumes using the Monte Carlo method with 10,000 random samples in the state space.

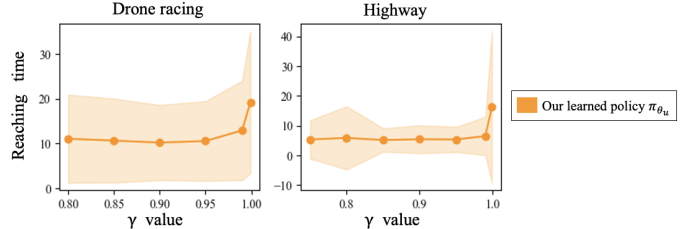


Figure 8: The average time taken for reaching the target set grows as  $\gamma$  increasing.

$\|x\|_2 \leq 0.1$ ) can safely reach the target set, under all potential disturbances. This enables real-time online certification.

### C. Hypothesis 3: The Lipschitz continuity of our new value function appears to accelerate learning

In Figure 6, we compare the critic loss (defined in (15) to measure the Bellman equation error) under different Bellman equations and time-discount factor  $\gamma$  values. Our critic loss converges rapidly when  $\gamma$  is chosen to ensure the Lipschitz continuity of our new value function.

### D. The trade-off of selecting a time-discount factor $\gamma$

We summarize our result in Figures 7 and 8. With a small  $\gamma$ , the learned RA sets can be conservative due to numerical errors, as an initial state whose optimal trajectory reaches the target set at a later stage may have near-zero time-discounted RA measures. However, the optimal policy tends to drive the state to the target set rapidly, as depicted in Figure 8. Conversely, a large  $\gamma$  can induce discontinuities in the value function, destabilizing learning and yielding suboptimal solutions. In the drone racing and highway experiments, we find that  $\gamma = 0.95$  ensures the Lipschitz continuity of  $V_\gamma(x)$ , thereby enhancing learning efficiency, and also mitigates unnecessary conservatism.

## IX. CONCLUSION AND FUTURE WORK

We propose a new framework for learning trustworthy reach-avoid (RA) sets. Our method features a newly designed RA value function that offers improved computational efficiency. We employ max-min DDPG to learn our value functions

and propose two efficient methods to certify whether a set of states can safely reach the target set with deterministic guarantees. We validate our methods through drone racing hardware experiments and highway take-over simulations. Our certification methods can be performed in real time, but they rely on offline value function learning beforehand. Future research may explore online reachability learning, as well as more efficient RA set certification methods.

## REFERENCES

- [1] C. Tomlin, G. J. Pappas, and S. Sastry, "Conflict resolution for air traffic management: A study in multiagent hybrid systems," *IEEE Transactions on Automatic Control*, vol. 43, no. 4, pp. 509–521, 1998.
- [2] K. Margellos and J. Lygeros, "Hamilton–jacobi formulation for reach–avoid differential games," *IEEE Transactions on Automatic Control*, vol. 56, no. 8, pp. 1849–1861, 2011.
- [3] J. F. Fisac, M. Chen, C. J. Tomlin, and S. S. Sastry, "Reach-avoid problems with time-varying dynamics, targets and constraints," in *Proceedings of the 18th international conference on hybrid systems: computation and control*, pp. 11–20, 2015.
- [4] R. Bellman, R. Corporation, and K. M. R. Collection, *Dynamic Programming*. Rand Corporation research study, Princeton University Press, 1957.
- [5] S. Bansal and C. J. Tomlin, "Deepreach: A deep learning approach to high-dimensional reachability," in *2021 IEEE International Conference on Robotics and Automation (ICRA)*, pp. 1817–1824, IEEE, 2021.
- [6] J. F. Fisac, N. F. Lugovoy, V. Rubies-Royo, S. Ghosh, and C. J. Tomlin, "Bridging hamilton–jacobi safety analysis and reinforcement learning," in *2019 International Conference on Robotics and Automation (ICRA)*, pp. 8550–8556, IEEE, 2019.
- [7] K.-C. Hsu, V. Rubies-Royo, C. J. Tomlin, and J. F. Fisac, "Safety and liveness guarantees through reach-avoid reinforcement learning," *arXiv preprint arXiv:2112.12288*, 2021.
- [8] K.-C. Hsu, A. Z. Ren, D. P. Nguyen, A. Majumdar, and J. F. Fisac, "Sim-to-lab-to-real: Safe reinforcement learning with shielding and generalization guarantees," *Artificial Intelligence*, vol. 314, p. 103811, 2023.
- [9] K.-C. Hsu, H. Hu, and J. F. Fisac, "The safety filter: A unified view of safety-critical control in autonomous systems," *Annual Review of Control, Robotics, and Autonomous Systems*, vol. 7, 2023.
- [10] K.-C. Hsu, D. P. Nguyen, and J. F. Fisac, "Isaacs: Iterative soft adversarial actor-critic for safety," in *Learning for Dynamics and Control Conference*, pp. 90–103, PMLR, 2023.
- [11] Z. Li, C. Hu, W. Zhao, and C. Liu, "Learning predictive safety filter via decomposition of robust invariant set," *arXiv preprint arXiv:2311.06769*, 2023.
- [12] A. Lin and S. Bansal, "Generating formal safety assurances for high-dimensional reachability," in *2023 IEEE International Conference on Robotics and Automation (ICRA)*, pp. 10525–10531, IEEE, 2023.
- [13] A. Lin and S. Bansal, "Verification of neural reachable tubes via scenario optimization and conformal prediction," in *6th Annual Learning for Dynamics & Control Conference*, pp. 719–731, PMLR, 2024.
- [14] D. P. Nguyen, K.-C. Hsu, W. Yu, J. Tan, and J. F. Fisac, "Gameplay filters: Robust zero-shot safety through adversarial imagination," in *8th Annual Conference on Robot Learning*, 2024.
- [15] A. A. Flem, M. Ghirardelli, S. T. Kral, E. Cheynet, T. O. Kristensen, and J. Reuder, "Experimental characterization of propeller-induced flow (pif) below a multi-rotor uav," *Atmosphere*, vol. 15, no. 3, p. 242, 2024.
- [16] D. Bertsekas, *Dynamic programming and optimal control: Volume 1*, vol. 4. Athena scientific, 2012.
- [17] A. Singh, Z. Feng, and S. Bansal, "Imposing exact safety specifications in neural reachable tubes," *arXiv preprint arXiv:2404.00814*, 2024.
- [18] H. H. Nguyen, T. Zieger, S. C. Wells, A. Nikolakopoulou, R. D. Braatz, and R. Findeisen, "Stability certificates for neural network learning-based controllers using robust control theory," in *2021 American Control Conference (ACC)*, pp. 3564–3569, IEEE, 2021.
- [19] M. Korda, "Stability and performance verification of dynamical systems controlled by neural networks: algorithms and complexity," *IEEE Control Systems Letters*, vol. 6, pp. 3265–3270, 2022.
- [20] R. Schwan, C. N. Jones, and D. Kuhn, "Stability verification of neural network controllers using mixed-integer programming," *IEEE Transactions on Automatic Control*, 2023.
- [21] S. Coogan, "Mixed monotonicity for reachability and safety in dynamical systems," in *2020 59th IEEE Conference on Decision and Control (CDC)*, pp. 5074–5085, IEEE, 2020.
- [22] T. Lew and M. Pavone, "Sampling-based reachability analysis: A random set theory approach with adversarial sampling," in *Conference on robot learning*, pp. 2055–2070, PMLR, 2021.
- [23] M. Everett, G. Habibi, and J. P. How, "Efficient reachability analysis of closed-loop systems with neural network controllers," in *2021 IEEE International Conference on Robotics and Automation (ICRA)*, pp. 4384–4390, IEEE, 2021.
- [24] H. Hu, M. Fazlyab, M. Morari, and G. J. Pappas, "Reach-sdp: Reachability analysis of closed-loop systems with neural network controllers via semidefinite programming," in *2020 59th IEEE Conference on Decision and Control (CDC)*, pp. 5929–5934, IEEE, 2020.
- [25] Y. Kwon, J. Michaux, S. Isaacson, B. Zhang, M. Ejakov, K. A. Skinner, and R. Vasudevan, "Conformalized reachable sets for obstacle avoidance with spheres," in *CoRL Workshop on SAFE-ROL*.
- [26] S. Prajna and A. Jadbabaie, "Safety verification of hybrid systems using barrier certificates," in *International Workshop on Hybrid Systems: Computation and Control*, pp. 477–492, Springer, 2004.
- [27] R. Mazouz, K. Muvvala, A. Raheesh Babu, L. Laurenti, and M. Lahijanjan, "Safety guarantees for neural network dynamic systems via stochastic barrier functions," *Advances in Neural Information Processing Systems*, vol. 35, pp. 9672–9686, 2022.
- [28] W. Xiao, T.-H. Wang, R. Hasani, M. Chahine, A. Amini, X. Li, and D. Rus, "Barriernet: Differentiable control barrier functions for learning of safe robot control," *IEEE Transactions on Robotics*, 2023.
- [29] A. D. Ames, X. Xu, J. W. Grizzle, and P. Tabuada, "Control barrier function based quadratic programs for safety critical systems," *IEEE Transactions on Automatic Control*, vol. 62, no. 8, pp. 3861–3876, 2016.
- [30] A. Taylor, A. Singletary, Y. Yue, and A. Ames, "Learning for safety-critical control with control barrier functions," in *Learning for Dynamics and Control*, pp. 708–717, PMLR, 2020.
- [31] Z. Qin, K. Zhang, Y. Chen, J. Chen, and C. Fan, "Learning safe multi-agent control with decentralized neural barrier certificates," in *International Conference on Learning Representations*, 2021.
- [32] J. Richalet, "Algorithmic control of industrial processes," *Proc. of the 4<sup>th</sup> IFAC Sympo. on Identification and System Parameter Estimation*, pp. 1119–1167, 1976.
- [33] B. T. Lopez, J.-J. E. Slotine, and J. P. How, "Dynamic tube mpc for nonlinear systems," in *2019 American Control Conference (ACC)*, pp. 1655–1662, 2019.
- [34] J. Achiam, D. Held, A. Tamar, and P. Abbeel, "Constrained policy optimization," in *International conference on machine learning*, pp. 22–31, PMLR, 2017.
- [35] Y. Chow, O. Nachum, A. Faust, E. Duenez-Guzman, and M. Ghavamzadeh, "Lyapunov-based safe policy optimization for continuous control," *arXiv preprint arXiv:1901.10031*, 2019.
- [36] Q. Yang, T. D. Simão, S. H. Tindemans, and M. T. Spaan, "Wcsac: Worst-case soft actor critic for safety-constrained reinforcement learning," in *Proceedings of the AAAI Conference on Artificial Intelligence*, vol. 35 Issue 12, pp. 10639–10646, 2021.
- [37] C. Tomlin, J. Lygeros, and S. Sastry, "Computing controllers for nonlinear hybrid systems," in *Hybrid Systems: Computation and Control: Second International Workshop, HSCC'99 Berg en Dal, The Netherlands, March 29–31, 1999 Proceedings 2*, pp. 238–255, Springer, 1999.
- [38] W. Giernacki, M. Skwierczyński, W. Witwicki, P. Wroński, and P. Kozierski, "Crazyflie 2.0 quadrotor as a platform for research and education in robotics and control engineering," in *the 22nd International Conference on Methods and Models in Automation and Robotics*, pp. 37–42, 2017.
- [39] L. Pichierri, A. Testa, and G. Notarstefano, "Crazychoir: Flying swarms of crazyflie quadrotors in ros 2," *IEEE Robotics and Automation Letters*, vol. 8, no. 8, pp. 4713–4720, 2023.
- [40] S. Bansal, M. Chen, S. Herbert, and C. J. Tomlin, "Hamilton-jacobi reachability: A brief overview and recent advances," in *2017 IEEE 56th Annual Conference on Decision and Control (CDC)*, pp. 2242–2253, IEEE, 2017.
- [41] H. Gouk, E. Frank, B. Pfahringer, and M. J. Cree, "Regularisation of neural networks by enforcing lipschitz continuity," *Machine Learning*, vol. 110, no. 2, pp. 393–416, 2021.
- [42] H. Xiong, T. Xu, L. Zhao, Y. Liang, and W. Zhang, "Deterministic policy gradient: Convergence analysis," in *Uncertainty in Artificial Intelligence*, pp. 2159–2169, PMLR, 2022.
- [43] S. Li, Y. Wu, X. Cui, H. Dong, F. Fang, and S. Russell, "Robust multi-agent reinforcement learning via minimax deep deterministic policy gradient," in *Proceedings of the AAAI conference on artificial intelligence*, vol. 33 Issue 1, pp. 4213–4220, 2019.